

Durham Research Online

Deposited in DRO:

25 November 2021

Version of attached file:

Accepted Version

Peer-review status of attached file:

Peer-reviewed

Citation for published item:

Alsafrani, Abdulrahmam and Parker, Mason and Shahbazi, Mahmoud and Horsfall, Alton (2021) 'High Gain DC-DC Multilevel Boost Converter to Enable Transformerless Grid Connection for Renewable Energy.', in 2021 56th International Universities Power Engineering Conference (UPEC). .

Further information on publisher's website:

<https://doi.org/10.1109/UPEC50034.2021.9548271>

Publisher's copyright statement:

© 2021 IEEE. Personal use of this material is permitted. Permission from IEEE must be obtained for all other uses, in any current or future media, including reprinting/republishing this material for advertising or promotional purposes, creating new collective works, for resale or redistribution to servers or lists, or reuse of any copyrighted component of this work in other works.

Additional information:

Use policy

The full-text may be used and/or reproduced, and given to third parties in any format or medium, without prior permission or charge, for personal research or study, educational, or not-for-profit purposes provided that:

- a full bibliographic reference is made to the original source
- a [link](#) is made to the metadata record in DRO
- the full-text is not changed in any way

The full-text must not be sold in any format or medium without the formal permission of the copyright holders.

Please consult the [full DRO policy](#) for further details.

High Gain DC-DC Multilevel Boost Converter to Enable Transformerless Grid Connection for Renewable Energy

Abdulrahman Alsafrani
Department of Engineering
Durham University
Durham, DH1 3LE, UK
Abdulrahman.e.alsafrani@durham.ac.uk

Mason Parker
Department of Engineering
Durham University
Durham, DH1 3LE, UK
Mason.parker@durham.ac.uk

Mahmoud Shahbazi
Department of Engineering
Durham University
Durham, DH1 3LE, UK
Mahmoud.shahbazi@durham.ac.uk

Alton Horsfall
Department of Engineering
Durham University
Durham, DH1 3LE, UK
Alton.b.horsfall@durham.ac.uk

Abstract— The solid state transformer (SST) is a new technology that will result in the replacement of traditional line frequency transformers in applications demanding high-power density and greater level of control. This paper describes a new form of boost converter to support the development of SST to enable the grid connection of renewable energy sources, such as wave energy and photovoltaics. SST contains the initial low voltage AC-DC converter, a high gain transformer based DC-DC converter, and the output high voltage DC-AC converter. A transformerless DC-DC Multilevel Boost Converter (MBC) is proposed, which combines the traditional boost converter with switched capacitor topology to realise a high voltage gain with only one driven switch and passive components. The main advantages of the proposed converter are the ability to realise high voltage gain without the need for an extreme (>80%) duty cycle, resulting in low voltage stress on the switching device and the creation of three self-balanced voltage levels at the output. The simulation results of the proposed topology are compared to the experimental results to validate the analyses. Thus, a 1 kW prototype MBC converter operating at 75 kHz is reported that resulted in a voltage gain of 10, with an experimental efficiency of 92.4% at a duty cycle of 71%, which compares favourably with the simulated efficiency of 94.5% under the same operating conditions.

Keywords—Solid state transformer (SST), multilevel Boost Converter (MBC), high voltage gain, continuous conduction mode (CCM).

I. INTRODUCTION

In the last two decades, the demand for higher renewable energy penetration has been growing rapidly to minimize the greenhouse gas emissions. Thus, the most significant consideration in electrical supply is to provide a clean, cheap, and sustainable supply of power to consumers through the distribution grid. To attain this goal, new technologies are required to enable efficient control, whilst offering increased reliability, and high levels of resilience at the grid level. One of the state-of-the-art technologies is the solid state transformer (SST), which has the potential to contribute to the integration of renewable energy to the distribution grid by enabling the grid connection of renewable energy sources. SST technology is a rapidly evolving topic, which is taking advantage of wide bandgap semiconductor devices and is not yet mature.

Significant research is being undertaken to assess the possibility of replacing the physically large line frequency magnetic transformer used in the distribution grid with SST circuits. SST topologies generally consist of multistage power electronics converters isolated with a high frequency transformer (HFT) which can control the input and output power, taking into account the voltage level using a number of switched electronic devices [1]. The main function of the SST is to facilitate the increase or decrease of the voltage, in a similar manner to the main function of a line frequency transformer.

A typical SST consists of an AC-DC rectifier, a DC-DC converter with HFT and a DC-AC inverter as shown schematically in figure 1 [2]. The fundamental operation of the SST is at first to rectify the 50 Hz AC voltage to DC. This DC voltage is stepped up using a DC-AC inverter, coupled to a HFT (with significantly decreased volume and weight in comparison to a 50 Hz transformer) before being rectified to give a DC voltage. Finally, the DC voltage it is converted into the desired 50 Hz AC voltage which connects to the distribution grid [3, 4]. The main advantage of SST over traditional LFT is the reduction in volume, which is dominated by the size of the transformer core and windings, which reduces as the cube of the operating frequency [5]. SST circuits have the ability to perform additional functionality with the help of semiconductor devices, including: protection circuits to prevent power supply and load disturbances, allow bidirectional flow, realise voltage sag compensation, as well as controlling the output voltage. The input circuits offer the possibility of having a DC input or output, increased voltage regulation, and fault isolation [6-8], as well as the ability to integrate power storage at the low and high voltage DC links.

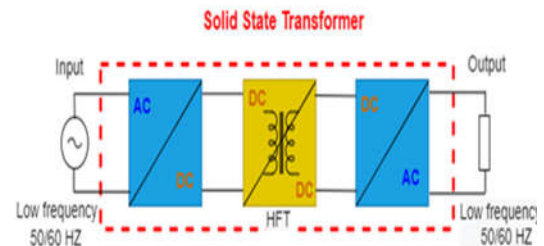


Figure 1. Schematic representation of a three stage SST.

The second stage of SST, which is identical in function to that of a high gain DC-DC converter, is the origin of the voltage boost. Thus, this paper focusses on the design of a high gain DC-DC converter, suitable for the integration of renewable energy sources to the distribution grid in the UK [9-19]. A voltage gain in excess of 5 is difficult to attain with traditional transformerless DC-DC boost converter topologies, due to the requirement for a duty cycle in excess of 80%, which results in significant losses in parasitic components [11, 12]. The use of a high switching frequency leads to a small size of the converter and suggests the use of wide bandgap semiconductor devices for the switch and diodes.

A transformerless DC-DC converter is a potential solution to the challenge of achieving a high voltage gain in a DC-DC converter. A number of topologies have been proposed in the literature for the realization of a transformerless DC-DC converter with high boost ratio and high efficiency [13]. These topologies, are generally complicated in comparison to the conventional DC-DC converter topology [9, 10], requiring a significant increase in the number of active devices and complex control strategies. The transformerless DC-DC multilevel boost converter (MBC) described here is a converter topology that combines the circuit of the traditional boost converter with a switched capacitor technique to generate a high voltage gain coupled with self-balancing outputs, that maintain the same output voltage for all output levels. This topology also, reduces the complexity of the control strategy by only requiring a single switching device, which is connected to ground, simplifying the gate drive requirements [9, 10]. The circuit controls the voltage by implementing pulse width modulation (PWM) using a single switch, one inductor, $(2N-1)$ diodes and $(2N-1)$ capacitors for obtaining an output which is N times that for a conventional boost converter operating under the same conditions.

The number of levels in the circuit and hence the output voltage can be increased by the addition of capacitors and diodes to the fundamental boost converter topology. This enables the circuit to be used as a power converter in applications where multiple controlled voltage levels with self-balancing are required when operating in a unidirectional current flow application [9]. Therefore, this transformerless DC-DC MBC circuits has the potential to be implemented in the middle stage of a three stage SST.

The paper is organized as follows; section II presents the converter topology and describes the modes of operation, section III analyzes the voltage gain of the proposed converter, section IV describes the influence of the component characteristics on the converter performance, section V outlines the performance of the converter using simulation and the validation of the model with experimental data to confirm the operating conditions, with the conclusion presented in section VI.

II. PROPOSED CONVERTER AND MODES OF OPERATION

A. Power Circuit

Figure 2 shows a schematic of the $N+1$ level DC-DC

MBC converter [9], which comprises, one switch, $(2N-1)$ diodes and $(2N-1)$ capacitors. In general, the converter topology is defined as having $N+1$ levels, which includes the zero level. The boost converter is PWM controlled at the gate contact of the power MOSFET, and has the potential to provide an equal voltage at all N output levels, denoted as V_c in the figure 2. The converter is based on a conventional DC-DC boost converter topology with the output voltage of the MBC is N times V_c , where V_c is the output voltage of the conventional converter. The other significant advantage of this topology for the realization of high voltages is the voltage stress on the components is lower than other proposed high voltage converter topologies, offering increased increasing the reliability, since each device blocks only one voltage level.

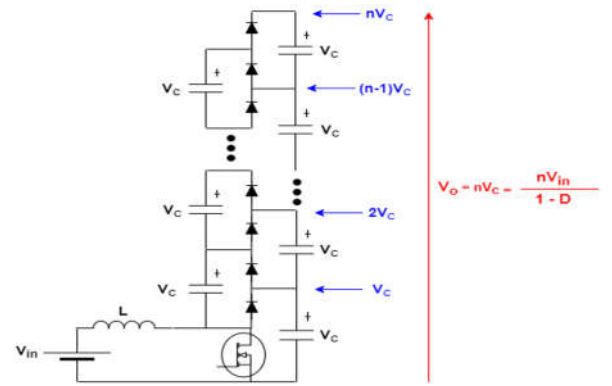


Figure 2. DC-DC MBC circuit for $N+1$ level

B. Operation Principle

The operating principle of the MBC can be described in terms of two operating modes; one when the switch is turned ON and the other when the switch is turned OFF. The converter has been designed to operate in continuous conduction mode (CCM) and the operating characteristics that occur during the two modes are described as follows:

In Mode 1, when the switch is turned ON, the inductor is connected to the input voltage, as indicated in Figure 3.a. If the voltage across C_2 is smaller than that across C_1 , C_1 charges C_2 through the diode D_2 and the switch, as indicated in Figure 3.b. At the same time, if the voltage across $C_2 + C_4$ is smaller than the voltage across $C_1 + C_3$, C_1 and C_3 charge C_2 and C_4 through the diode D_4 and the switch, as indicated in Figure 3.c [9].

In Mode 2, when the switch is turned OFF, the diode D_1 conducts allowing the energy stored in the magnetic field in the inductor charges capacitor C_1 until the voltage on this capacitor is equal to the voltage which is the sum of the input voltage and the inductor voltage, as shown in Figure 4.a. Then, diode D_3 conducts so the input voltage, the inductor and capacitor C_2 charge the capacitor C_1 and C_3 as indicated in Figure 4.b. When the voltage on $C_1 + C_3$ is equal to the total voltage on the input voltage, the inductor voltage and the voltage on the capacitor C_2 , diode D_3 turns off and diode D_5 conducts, so that the input voltage, inductor and capacitors C_2 and C_4 charge capacitors C_5, C_3, C_1 until the voltage is equal to the summation of the voltage on the input voltage, inductor and capacitors $C_2 + C_4$ as indicated in Figure 4.c [9].

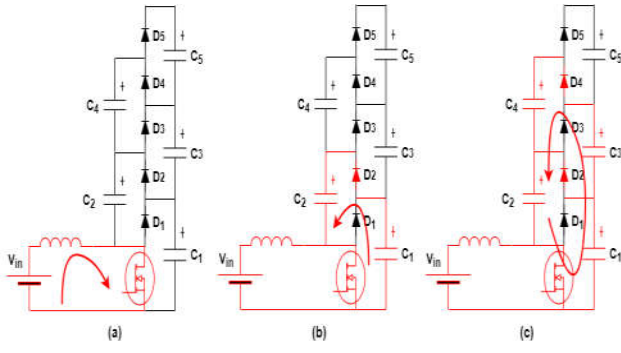


Figure 3. Operation of the MBC when the switch is ON

III. VOLTAGE GAIN OF THE PROPOSED CONVERTER

In the MBC circuit, the input power is transferred to the output by charging and discharging the switched-capacitor voltage doubler. The average voltage of the inductor for an idealised conventional boost converter, which is zero over a complete switching cycle, can be expressed [10]:

$$V_L = D(V_{in}) + (1 - D)(V_{in} - V_o) = 0 \quad (1)$$

Where V_L is the inductor voltage, V_{in} is the input voltage, V_o is the output voltage, and D is the duty cycle. Conventional analysis describes the steady state output voltage as:

$$\frac{V_o}{V_{in}} = \frac{1}{1 - D} \quad (2)$$

For the multilevel boost converter (MBC), when the switch is ON (operating in mode 1) the voltage drop across the inductor equals the input voltage. In Mode2, when the switch is OFF, the inductor voltage can be expressed as:

$$V_L = V_{in} - V_c \quad (3)$$

The inductor voltage can be determined by setting $V_L = V_{in}$ and equation (3),

$$V_L = D(V_{in}) + (1 - D)(V_{in} - V_c) = 0 \quad (4)$$

$$V_{in} = V_c(1 - D) \quad (5)$$

Since the voltage across all the output capacitors is identical V_c , the output voltage of the converter is $V_o = NV_c$. Hence the voltage gain of the proposed converter can be determined,

$$\frac{V_o}{V_{in}} = \frac{N}{1 - D} \quad (6)$$

In a real converter, the equivalent series resistance of the inductor ($R_{ESR,L}$) needs to be incorporated and so equation (4) can be modified to give:

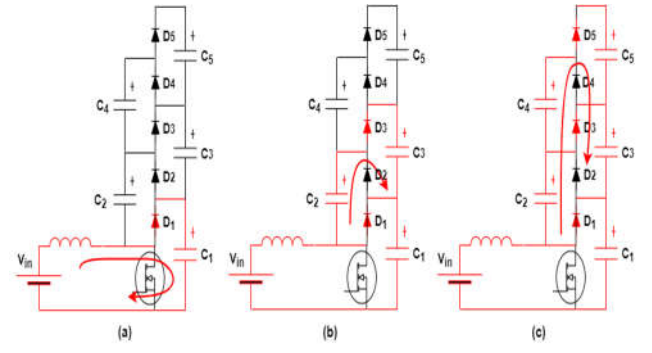


Figure 4. Operation of the MBC when the switch is OFF

$$V_L = D(V_{in} - I_L R_{ESR,L}) + (1 - D)(V_{in} - V_o - I_L R_{ESR,L}) = 0 \quad (7)$$

Then the gain conversion ratio can be expressed as:

$$\frac{V_o}{V_{in}} = \frac{1}{\frac{(1 - D)}{N} + \frac{N R_{ESR,L}}{(1 - D)R_o}} \quad (8)$$

It is clear from the analysis presented here that the inclusion of the inductor ESR reduces the voltage gain of the converter. In a practical converter this requires an increase in the duty cycle to achieve the desired output voltage.

IV. COMPONENT ANALYSIS

The discussions given here is based on the example of a 3-level boost converter, as shown in Figure 2.

A. Inductor

The inductor current I_L can be determined from the output current and the input and output voltages, under the assumption that $I_{in} = I_L$:

$$V_{in} I_{in} = V_o I_o$$

$$V_{in} I_L = V_o \frac{V_o}{R_o}$$

$$I_L = \frac{V_o}{V_{in}} \frac{V_o}{R_o} \quad (9)$$

Substituting the voltage gain from (6) into (9), the inductor current can be expressed as:

$$I_L = \frac{NV_o}{(1 - D) R_o} \quad (10)$$

Where I_{in} is the input current and R_o is the load resistance.

From equation (10), it is observed that the input current can be regulated by varying the value of the duty cycle D applied to the gate of the switch. The critical value of the inductance

that allows the converter to operate in continuous conduction mode (CCM) is determined using the duty cycle and output power, where f is the switching frequency, as expressed below:

$$L_{CRIT} = \frac{D(1-D)^2 R_o}{2f} \quad (11)$$

B. Capacitors

One of the significant features of the MBC is to maintain the same output voltage across each of the output capacitors, C_1, C_3 and C_5 . Under the assumption that all capacitors have the same capacitances, the following relationships are established and the output voltage across the load will be:

$$V_{C1} = V_{C3} = V_{C5} = V_C \rightarrow V_o = 3V_C \quad (12)$$

The design consideration for capacitors is that the voltage ripple should not exceed 5% and so, the capacitance can be determined from ΔV_o , the voltage ripple of capacitor.

$$C = \frac{D}{R_o \left(\frac{\Delta V_o}{V_o} \right) f} \quad (13)$$

C. Switch

According to the data shown in Figure 4(a), the voltage across the switch, V_S , in the proposed converter can be expressed as:

$$V_S = V_{C1} \quad (14)$$

By substituting equation (12) into (14) the voltage stress experienced by the switch in the three level converter is found to be lower than that for a converter with an equivalent output voltage and may be expressed as

$$V_S = \frac{V_o}{3} \quad (15)$$

V. SIMULATION AND EXPERIMENTAL RESULTS

The initial design has been simulated using LTSpice to validate the values for the passive components calculated using the analysis specified in section IV and to examine the switching transients in the circuit. Following the intention for the circuit to be used as part of a Solid State Transformer (SST) to enable renewable energy integration with the distribution grid, the specifications of the MBC are shown in table I. Simulated characteristics of a three-level boost converter have been used to boost a DC input voltage of 100 V to an output of 1000 V. To ensure an adequate portion of the operating period with the switch turned off, in order to avoid excessive voltage stress whilst achieving a gain factor of 10, the duty cycle was not allowed to exceed 75%. Following the analysis in the previous section, a three level

Table I. Design specification of MBC

Parameter	Symbol	Value
Input Voltage	V_{in}	100 V
Output Voltage	V_o	1000 V
Output Power	P_o	1 kW
Switching Frequency	f	75 kHz
Duty Cycle	D	0.71
Inductor	L	500 μH
Capacitors	$C_1 - C_7$	5 μF

converter was investigated and a duty cycle of 71% found to give an output voltage of 1 kV with an output power of 1 kW.

A hardware prototype of the proposed converter was built to test and validate the simulation based models. A commercial Silicon Carbide MOSFET (Infineon part number IMW120R030M1HXKSA1) was chosen as the power switch, which has an on-state resistance ($R_{ds(ON)}$) of 0.03 Ω and a blocking voltage of 1200 V. All the diodes in the circuit are Silicon Carbide Schottky Diodes (ST Microelectronics part number STPSC15H12WL) with a forward voltage drop of 1.35 V.

The voltage gain of the proposed converter is plotted as a function of the duty cycle as depicted in Figure 5. The data in the figure shows a comparison among the ideal case, theoretical results, and simulation results. It can be noticed that for duty cycle less than 0.7, the voltage gain conversion ratios of the three cases have no much difference. However, for a duty cycle greater than 0.7, a big difference can be seen between the ideal case and the theoretical and simulation results due to the effect of the inductor ESR.

The efficiency of the proposed converter was evaluated as a function of the switching frequency between 25 and 200 kHz, in order to determine the maximum operating point and optimum efficiency for this converter topology. The efficiency is directly calculated by measuring the input and output powers. The data show a maximum simulated efficiency of 94.5%, when the converter was operated at 75 kHz with a duty cycle of 71%, as shown by the blue data set in Figure 6.

In comparison to the simulation data, the performance of the experimental converter shows two distinct deviations as depicted by the red data set in Figure 6. Firstly, the efficiency of the converter is decreased by an average of 3.0%, from

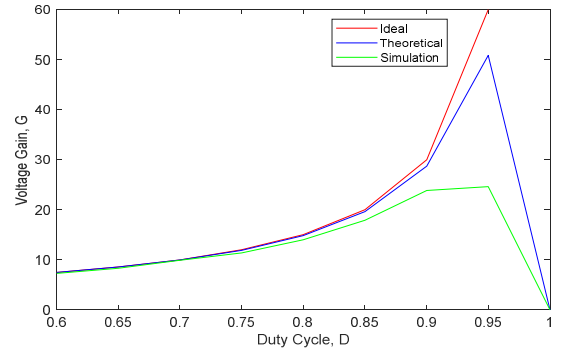


Figure 5. Ideal, theoretical and simulation of voltage gain against duty cycle for the MBC.

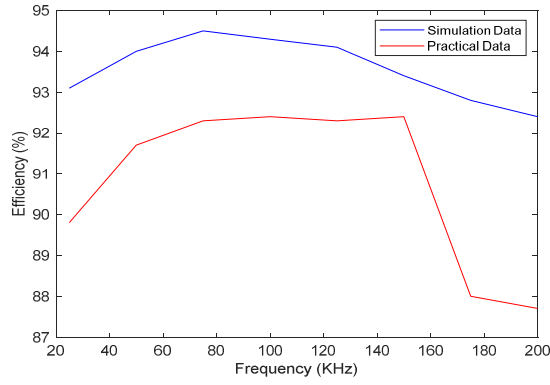


Figure 6. Simulation and practical efficiency of the proposed converter.

93.7% to 90.7%. Secondly, instead of the peak efficiency being observed at 75 kHz, a smaller variation with frequency is observed, with the variation ranging between 91.7% and 92.4% over the frequency range between 50 and 150 kHz. This indicates that the switching frequencies in this range can be operated as though they are the maximum operating points.

The data in figures 7, 8 and 9 show the simulation and experimental waveforms for the converter operating at 75 kHz. In general, the experimental waveforms show a high level of agreement with the waveforms from the SPICE simulations. The input voltage and output voltage waveforms are shown in Figure 7. The simulation and experimental results confirm the ability of the equations presented in this paper to determine the voltage gain of the three level DC-DC boost converter. It can be observed from the data that the experimental waveforms show switching transients that are not evident in the simulation results. The input voltage transients, which occur at the turn on and turn off transients of the switch, originate in the parasitic capacitances and inductances in the circuit. The output voltage transients are related to the input transients being propagated through the circuit.

The data in Figure 8 shows the variation in input current, which is the inductor current, and output current. The data in the figure confirms that the converter is operating in CCM, as predicted by the analysis presented in this paper. The voltage across the inductor and switch during operation are shown in Figure 9. The experimental inductor and switch voltages are close to those calculated and extracted from the simulation waveforms. The experimental inductor voltages are measured to $V_{LSON} = 100\text{ V}$ and $V_{LSOFF} = -250\text{ V}$ when the switch is turned ON and OFF respectively, which are closed to calculated and simulated values of $V_{LSON} = 100\text{ V}$, $V_{LSOFF} = -233\text{ V}$ and $V_{LSON} = 100\text{ V}$, $V_{LSOFF} = -245\text{ V}$ respectively.

The data confirm that a high voltage gain can be accomplished using this converter topology which confirms the suitability of this topology in this application. Moreover, the main advantage of proposed converter is to reduce the voltage stress on the switch. Equation 15 gives a predicted maximum drain-source voltage across the switch of 333 V when the output voltage is 1000V. Hence, the experimental and simulation switching voltage of $V_S = 350\text{ V}$ and $V_S = 345\text{ V}$ respectively is closed to the estimated value. The experimental waveforms validate the proposed converter theoretical and simulation.

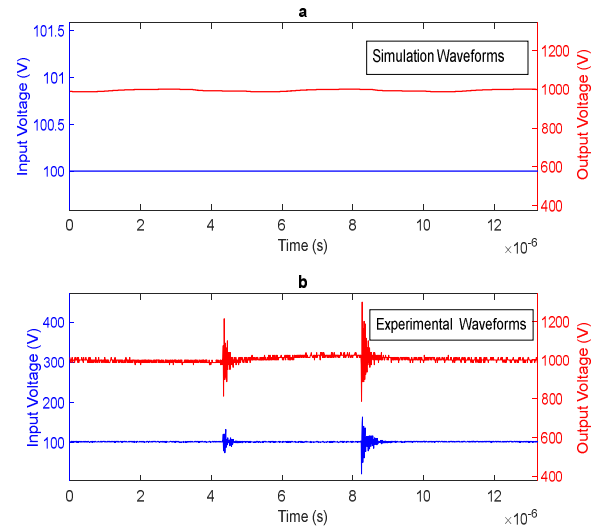


Figure 7. Input and output voltage waveforms of the MBC, (a) simulation and (b) Experimental.

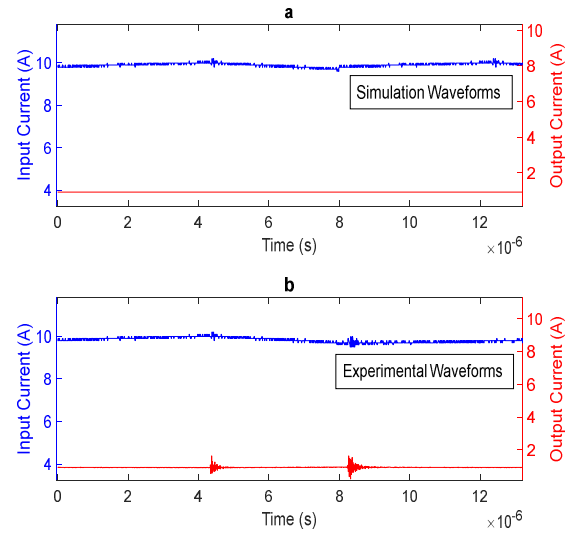


Figure 8. Input and output current waveforms of the MBC, (a) simulation and (b) Experimental.

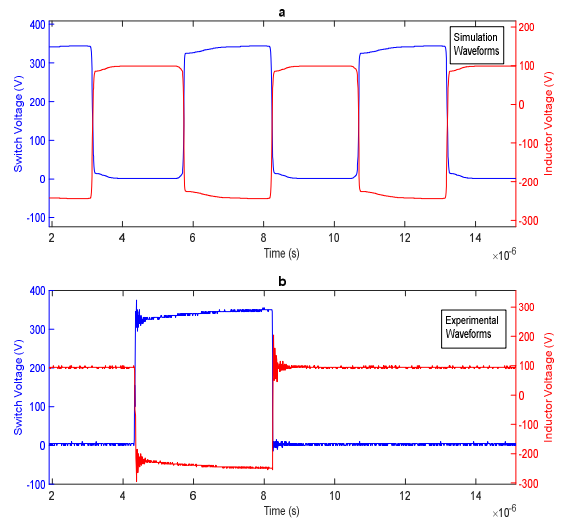


Figure 9. Switch voltage and inductor voltage waveforms of the MBC, (a) simulation and (b) Experimental.

The power ratings of the selected components in the hardware prototype were used to conduct a theoretical loss analysis. The percentage distribution of losses in the proposed converter is depicted in Figure 10. It is concluded that the major percent of losses occurs in the switch which is about 63.53%. Then, the diodes account for about 22.7% of the losses. After that, around 10.41% of the losses comes from the inductor. Finally, the losses in the capacitors are 3.38% which are very small as the ESR of the film capacitors used is in the order of few milliohms and the rms currents are around 10A. Hence, at 1kW, the estimated efficiency is around 94.5%. A 1kW prototype was built and tested to validate the analytical and simulation results. An efficiency of 92.4% was observed at 150KHz. The core losses in the inductor that is not included in the estimated efficiency, as well as the approximate approach to calculate the component losses, can be accounted for the difference between the calculated and experimental efficiency. In addition, the parasitic capacitances and inductances in the circuit that cause the switching transients of input and output voltage, as shown in Figure 7(b), can influence the experimental efficiency.

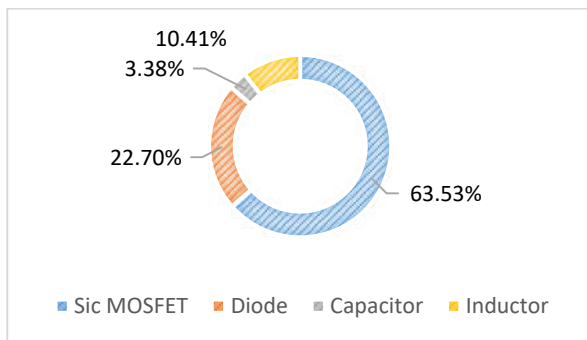


Figure 10. Percentage distribution of losses in the proposed converter

VI. CONCLUSION

In this paper, a high-voltage-gain DC-DC multilevel boost converter (MBC) is described that can offer a voltage gain of 10 without the need for complex multi-switch control algorithms or high voltage stress on the switch. The proposed converter topology combines the conventional boost converter topology with a switched capacitor circuit, which comprises one inductor, one switch, (2N-1) diodes and (2N-1) capacitors for an N-level converter. The major advantages of the proposed converter are that it offers a low voltage stress across the switch, continuous input current, and a high voltage gain without the need for an excessive duty cycle. The experimental results of the proposed converter with an input voltage of 100 V show an output voltage of 1000 V at 1 kW. The experimental efficiency of the converter is 92.4% when operated at a switching frequency of 150 kHz. Simulations of the circuits show a good level of match with the experimental data in terms of the trends in the operating conditions. The data presented confirm the theoretical analysis developed for the circuit with parasitic components and identify that the transformerless DC-DC MBC is suitable for the middle stage of SST for renewable energy integration.

References

[1] M. M. Samad, "Solid State Transformers: The State-of-the-Art, Challenges and Applications," *Proceedings of the World*

congress on Engineering 2019, WCE 2019, July 3-5, 2019, London, U.K.

[2] A. Q. H. Xu She, Rolando Burgos, "Review of solid-state transformer technologies and their application in power distribution systems," *IEEE journal of emerging and selected topics in power electronics*, vol. 1, no. 3, pp. 186-198, 2013.

[3] R. B. Xu She, Gangyao Wang, Fei Wang, Alex Q Huang, "Review of solid state transformer in the distribution system: From components to field application," in *IEEE Energy Conversion Congress and Exposition (ECCCE)*, 2012, pp. 4077-4084.

[4] A. P. C. d. M. Rodolfo P. Londero, and Guilherme S. da Silva, "Comparison between conventional and solid state transformers in smart distribution grids," in *IEEE PES Innovative Smart Grid Technologies Conference-Latin America (ISGT Latin America)*, 2019: IEEE, pp. 1-6.

[5] M. G. L. Gabriel Ortiz, Jonas Emanuel Huber, and Johann Walter Kolar, "Design and experimental testing of a resonant DC-DC converter for solid-state transformers," *IEEE Transactions on Power Electronics*, vol. 32, no. 10, pp. 7534-7542, 2016.

[6] H. d. T. M. JW Van Der Merwe, "The solid-state transformer concept: A new era in power distribution," in *AFRICON 2009: IEEE*, pp. 1-6.

[7] S. K. G. Mohammed Ovais Ansari, and Sushma Gupta, "Solid state transformer with a LC filter for distribution network," in *International Conference on Innovations in Control, Communication and Information Systems (ICICCI)*, 2017: IEEE, pp. 1-6.

[8] G. G. a. J. A. Martinez-Velasco, "A solid state transformer model for power flow calculations," *International Journal of Electrical Power & Energy Systems*, vol. 89, pp. 40-51, 2017.

[9] J. M. R. Julio C. Rosas-Caro, Pedro Martín García-Vite, "Novel DC-DC multilevel boost converter," in *IEEE Power Electronics Specialists Conference*, 2008: IEEE, pp. 2146-2151.

[10] J. M. R. J.C. Rosas-Caro, F.Z. Peng, and A. Valderrabano, "A DC-DC multilevel boost converter," *IET Power Electronics*, vol. 3, no. 1, pp. 129-137, 2010.

[11] J. C. R.-C. Jonathan C. Mayo-Maldonado, Rubén Salas-Cabrera, Aarón González-Rodríguez, Omar F. Ruiz-Martínez, Rafael Castillo-Gutiérrez, Jesus R. Castillo-Ibarra, and Hermenegildo Cisneros-Villegas, "State space modeling and control of the dc-dc multilevel boost converter," in *20th International Conference on Electronics Communications and Computers (CONIELECOMP)*, 2010: IEEE, pp. 232-236.

[12] J. M. R. Julio C. Rosas-Caro, and Antonio Valderrabano, "Voltage balancing in DC/DC multilevel boost converters," in *40th North American Power Symposium*, 2008: IEEE, pp. 1-7.

[13] J. C. M.-M. Julio Cesar Rosas-Caro, Ruben Salas-Cabrera, Aaron Gonzalez-Rodriguez, Eduardo Nacu Salas-Cabrera, and Rodolfo Castillo-Ibarra, "A family of DC-DC multiplier converters," *Engineering Letters*, vol. 19, no. 1, pp. 57-67, 2011.

[14] D. V. A. K. S. Nagaraja Rao, and Ch. Sai Babu, "Grid Connected Distributed Generation System with High Voltage Gain Cascaded DC-DC Converter Fed Asymmetric Multilevel Inverter Topology," *International Journal of Electrical & Computer Engineering (2088-8708)*, vol. 8, 2018.

[15] M.-K. N. Van-Thuan Tran, Youn-Ok Choi, and Geum-Bae Cho, "Switched-capacitor-based high boost DC-DC converter," *Energies*, vol. 11, no. 4, p. 987, 2018.

[16] D. d. C. P. Fernando Lessa Tofoli, Wesley Josias de Paula, and Demercil de Sousa Oliveira Júnior, "Survey on non-isolated high-voltage step-up dc-dc topologies based on the boost converter," *IET power Electronics*, vol. 8, no. 10, pp. 2044-2057, 2015.

[17] H. A. Alya Al-Hafri, Amer Ghias, and Qassim Nasir, "Transformer-less based solid state transformer for intelligent power management," in *5th International Conference on Electronic Devices, Systems and Applications (ICEDSA)*, 2016: IEEE, pp. 1-4.

[18] Y. B. B. Axelrod, A. Shenkman, and G. Golan, "Diode-capacitor voltage multipliers combined with boost-converters: Topologies and characteristics," *IET Power Electronics*, vol. 5, no. 6, pp. 873-884, 2012.

[19] S. M. Gang Wu, Xinbo Ruan, Senior Member, and Zhihong Ye, "Nonisolated high step-up DC-DC converters adopting switched-capacitor cell," *IEEE Transactions on Industrial Electronics*, vol. 62, no. 1, pp. 383-393, 2014.